Structure−Property Relationships in Light-Emitting Polymers: Optical, Electrochemical, and Thermal Studies

Min Zheng,[†] Ananda M. Sarker,[†] E. Elif Gürel,[†] Paul M. Lahti,[‡] and Frank E. Karasz*[,†]

Department of Polymer Science & Engineering and Department of Chemistry, University of Massachusetts, Amherst, Massachusetts 01003

Received May 18, 2000; Revised Manuscript Received July 31, 2000

ABSTRACT: A series of new PPV-based alternating copolymers containing conjugated and nonconjugated blocks have been synthesized with the objective of raising the glass transition temperature (T_g) relative to structures previously obtained. The higher T_g was achieved by inserting a more rigid unit in the spacer soft block. The effects of molecular architecture and chromophore substituents on the optical and redox properties of the polymers were investigated. The UV−vis absorption and emission in the solid state were in the range 360−415 and 455−533 nm, respectively. The calculated band gaps using cyclic voltammetry data were in the range 2.41−3.30 eV and were in good agreement with those calculated from the UV−vis spectra edge. The results show that, through a choice of substituents and backbone structure, the emission color and other properties can be systematically varied.

Introduction

It has been shown previously that PPV-related copolymers containing aromatic conjugated and aliphatic nonconjugated blocks are soluble, have good film-forming and mechanical properties and are suitable for fabrication of light-emitting devices.[1−4] These alternating block copolymers provide efficient exciton confinement because of a microphase-separated domain structure,[5] and by appropriate selection of chromophores, they can provide emission at any selected portion of the spectrum. Such copolymers (Scheme 1) have shown to be efficient light-emitting electroluminescent materials in several LED architectures.[1−4] The copolymers reported to date have single glass transition temperatures (T_g) about 50 °C above ambient.[2,5] The present study is focused on the synthesis and properties of copolymers with well-defined conjugated chromophore segments and with a *m*-xylene spacer unit in the soft block (Scheme 2, polymers **2a**−**h**). The effect of the *m*-xylene block on the T_g and of selected substituents on the chromophore unit, as well as architectural variations in chromophores, was investigated by optical, thermal, and electrochemical techniques.

Experimental Section

Melting points were taken on a Fisher-Johns melting point apparatus and are uncorrected. NMR spectra were collected on a Bruker DPX300 spectrometer in chloroform-*d* solvent with tetramethylsilane (TMS) as internal standard. Elemental analysis was carried out in the University of Massachusetts Microanalytical Laboratory. FTIR spectra were recorded on IBM IR/3X type 913X FTIR spectrometer. UV−vis spectra were recorded on an IBM 9420 spectrometer. Emission spectra were obtained on a Perkin-Elmer LS 50B spectrometer with a xenon lamp as light source and were corrected in the usual manner. The relative emission quantum yields were determined using 9,10-diphenylanthracene in cyclohexane as standard ($\Phi_f = 0.90$).[6] Differential scanning calorimetry (DSC) was run on a Perkin-Elmer DSC-7 using Pyris software; indium and tin were used for calibration. The glass transition temperatures reported were taken as the onset temperature of the heat capacity discontinuity. The molecular weights of polymers were determined by gel permeation chromatography with THF as eluent and polystyrene as standard. Cyclic voltammetry (CV) was performed using an EG&G model 362 potentiostat under nitrogen atmosphere. Platinum (Pt) wire electrodes were used as both counter and working electrodes, and a silver electrode was used as reference. The films on the working electrode were prepared by dipping the Pt wire into a concentrated polymer solution (2 wt %, chloroform) and drying in a vacuum for 2 h. CV measurements were done in an electrolyte solution of 0.1 M tetrabutylammonium tetrafluoroborate (Bu_4NBF_4) in acetonitrile.

Scheme 1. Structure of Reference Polymer 1

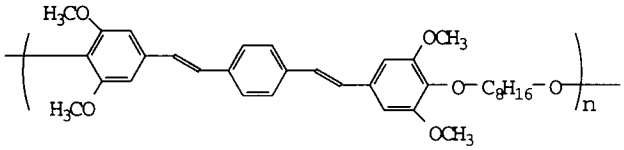

1,3-Bis(2,6-dimethoxy-4-formylphenoxy)xylene (3). A mixture of 3,5-dimethoxy-4-hydroxybenzaldehyde (1.82 g, 10 mmol), α,α′-*m*-xylylene dichloride (0.93 g, 5 mmol), and potassium carbonate (1.2 g, 11.3 mmol) in anhydrous dimethylformamide (50 mL) was heated to 80 °C under nitrogen for 12 h. The mixture was cooled to room temperature and poured into ice−water (150 mL). The white precipitate was collected, washed with water, and recrystallized twice from ethanol. The product was obtained as white crystals (yield 50%); mp 109−110 °C. ^{1}H NMR ($CDCl_3$, δ): 9.87 (s, 2 H), 7.6 (s, 1 H), 7.4 (d, 2 H), 7.3 (m, 1 H), 7.12 (s, 4 H), 5.12 (s,4 H), 3.9 (s, 12 H). Elemental calcd. for $C_{26}H_{26}O_8$: C, 66.95; H, 5.58. Found: C, 66.75; H, 5.45.

Intermediates 4b−**h**. 2,5-Dimethyl-*p*-xylylenebis(triphenylphosphonium chloride) (**4b**),[7] 2,5-dimethoxy-*p*-xylylenebis(triphenylphosphonium chloride) (**4c**),[8] 2,5-dihexadecyloxy-*p*-xylylenebis(triphenylphosphonium bromide) (**4d**),[9] *m*-xylylenebis(triphenylphosphonium bromide) (**4g**),[8] and 9,10-anthrylenedimethylenebis(triphenylphosphonium chloride) (**4h**)[10] were synthesized according to published procedures.

2-Fluoro-*p*-xylylenebis(triphenylphosphonium bromide) (4e). The synthesis were carried out by heating a mixture of triphenylphosphine (4.20 g, 16.0 mmol) and 1,4-

[†] Department of Polymer Science & Engineering.
[‡] Department of Chemistry.
* To whom all correspondence should be addressed. E-mail: fekarasz@polysci.umass.edu.

10.1021/ma000865x CCC: $19.00
Published on Web 09/09/2000

Scheme 2. Syntheses of Polymer 2a−h

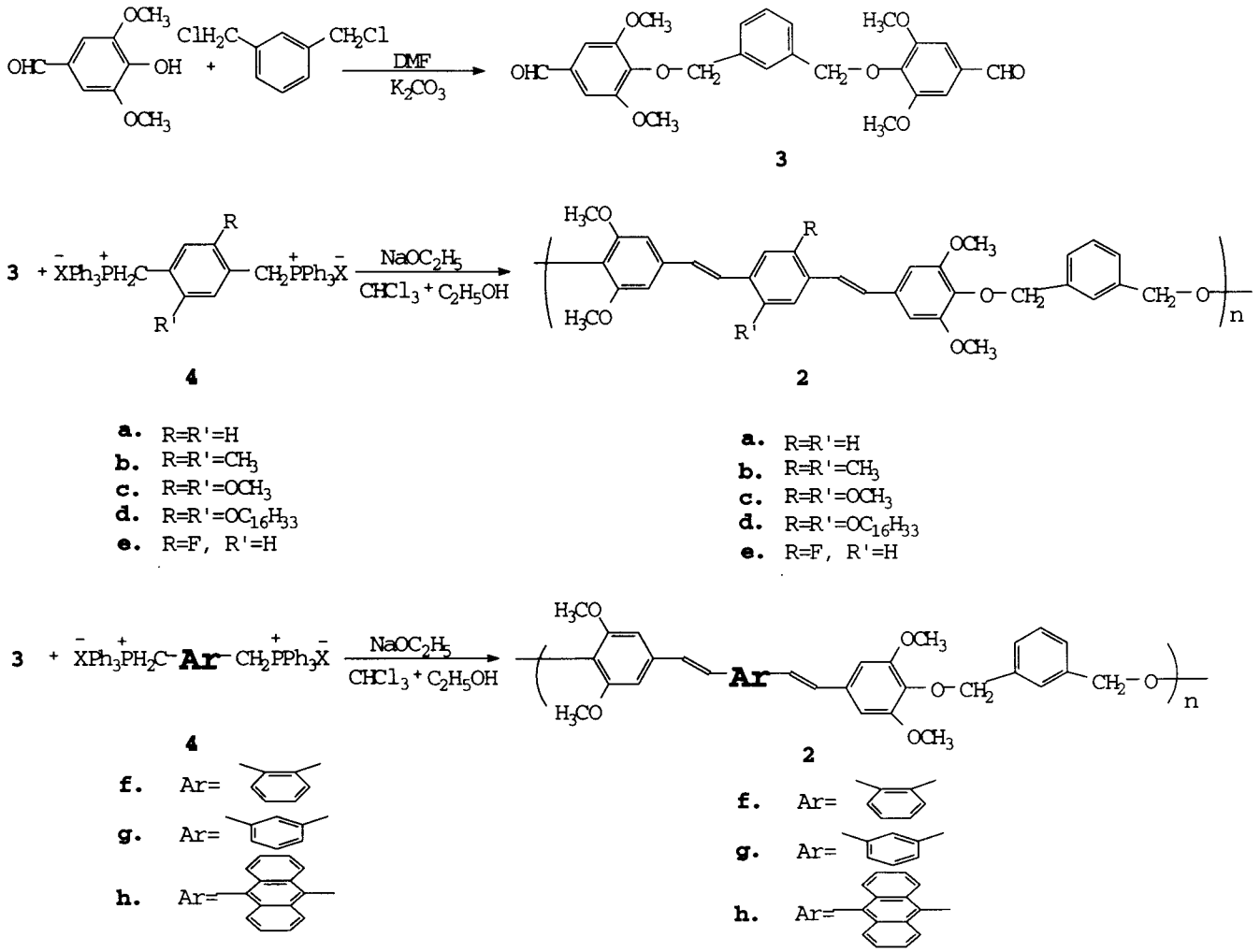

bis(bromomethyl)-2-fluorobenzene (2.0 g, 7.14 mmol)[11] in dimethylformamide (50 mL) at 105−110 °C under nitrogen overnight. The product was obtained as a precipitate, leaving unreacted starting materials and monosubstituted phosphonium salt in solution. The product was filtered followed by washing with diethyl ether (100 mL) to give the phosphonium salt as a white powder (67% yield); mp > 200 °C. ^{1}H NMR (CD_3OD, δ): 7.97−7.87 (m, 6 H), 7.81−7.72 (m, 24 H), 7.03−6.97 (m, 1 H), 6.77 (d, 2 H), 5.11 (d, 2 H), 5.04 (d, 2 H). Elemental calcd. for $C_{44}H_{37}Br_2FP_2$: C, 65.53; H, 4.62; Br, 19.81; P, 7.69. Found: C, 65.70; H, 4.52; Br, 19.72; P, 7.52.

General Procedure for Polymerization.[2] A solution of sodium in anhydrous ethanol (3 mol excess with respect to monomers) was added dropwise at ambient temperature under nitrogen to a mixture of equal molar amounts of dialdehyde and phosphonium salt in anhydrous ethanol and dry chloroform (2.5:1). The mixture was stirred at room temperature overnight. Polymerization was quenched by adding dilute hydrochloric acid (2% in water) and stirring for a few minutes. The resultant material was dissolved in a minimum amount of chloroform and was added dropwise to ethanol while stirring to precipitate the polymer. The dried polymer was dissolved in toluene, a catalytic amount of iodine was added, and the reaction refluxed overnight under a nitrogen atmosphere. After cooling, the toluene was removed under reduced pressure, and the residue was then dissolved in chloroform and reprecipitated into 90% ethanol. Reprecipitation was performed four times on the isomerized polymeric product, which was subsequently dried under vacuum at 40 °C. Copolymer yields typically ranged from 30 to 50%.

Copolymer 2a: ^{1}H NMR ($CDCl_3$, δ): 7.6 (s, 1 H), 7.4 (s, 4 H), 7.3 (d, 2 H), 7.2 (m, H), 6.9 (d, 4 H), 6.65 (s, 4 H), 4.98 (s, 4 H), 3.9 (s, 12 H). FTIR (KBr, cm^{-1}): 3024, 2960, 2910, 2863, 2824, 1580, 1504, 1464, 1420, 1327, 1236, 1128, 960. Elemental calcd. for $(C_{34}H_{32}O_6)$n: C, 76.11; H, 5.97. Found: C, 75.42; H, 5.99.

Copolymer 2b: ^{1}H NMR ($CDCl_3$, δ) 7.6(s, 1 H), 7.5(m, 3 H), 7.3(s, 2 H), 7.2(d, 2 H), 6.9(d, 2 H), 6.7(s, 4 H), 5.0(s, 4 H), 3.9(s, 12 H), 2.4(s, 6 H). FTIR (KBr, cm^{-1}), 3005, 2963, 2920, 2874, 2824, 1582, 1505, 1464, 1419, 1327, 1238, 1126, 960, 756, 667. Elemental calcd. for $(C_{36}H_{36}O_6)_n$: C, 76.60; H, 6.38. Found: C, 75.92; H, 6.27.

Copolymer 2c: ^{1}H NMR ($CDCl_3$, δ) 7.6 (s, 1 H), 7.5 (m, 3 H), 7.4 (s, 2 H), 7.1 (d, 2 H), 6.9 (d, 2 H), 6.7 (s, 4 H), 5.0 (s, 4 H), 4.1 (s, 6 H), 3.9 (s, 12 H). FTIR (KBr, cm^{-1}): 3008, 2958, 2920, 2854, 2810, 1560, 1505, 1462, 1419, 1327, 1238, 1128, 960. Elemental calcd. for $(C_{36}H_{36}O_8)_n$: C, 72.48; H, 6.04. Found: C, 71.16; H, 5.97.

Copolymer 2d: ^{1}H NMR ($CDCl_3$, δ): 7.6 (s, 1 H), 7.5 (m, 3 H), 7.4 (s, 2 H), 7.1 (d, 2 H), 6.9 (d, 2 H), 6.7 (s, 4 H), 5.0 (s, 4 H), 4.1 (t, 4 H), 3.9 (s, 12 H), 1.8 (m, 4 H), 1.55 (m, 4 H), 1.2 (m, 48 H), 0.9 (t, 6 H). FTIR (KBr, cm^{-1}): 3010, 2955, 2920, 2851, 2808, 1558, 1504, 1462, 1420, 1325, 1238, 1126, 960. Elemental calcd. for $(C_{66}H_{96}O_8)_n$: C, 77.95; H, 9.45. Found: C, 76.46; H, 9.21.

Copolymer 2e: ^{1}H NMR ($CDCl_3$, δ): 7.5−7.6 (m, 2 H), 7.4 (m, 3 H), 7.2−7.1 (m, 4 H), 7.0−6.9 (d, 2 H), 6.7 (s, 4 H), 4.96 (s, 4 H), 3.9 (s, 12 H). FTIR (KBr, cm^{-1}): 3005, 2960, 2917, 2820, 1582, 1505, 1462, 1419, 1327, 1238, 1126, 960. Elemental calcd. for $(C_{34}H_{31}FO_6)_n$: C, 73.78; H, 5.61. Found: C, 72.44; H, 5.62.

Copolymer 2f: ^{1}H NMR ($CDCl_3$, δ): 7.5−7.6 (m, 2 H), 7.4−7.3 (m, 3 H), 7.2 (m, 3 H), 6.9 (m, 2 H), 6.7 (s, 2 H), 6.6 (s, 2 H), 6.4 (d, 2 H), 5.0 (s, 4 H), 3.8 (s, 9 H), 3.5 (s, 3 H). FTIR

Table 1. Molecular Weight and Thermal Properties of Copolymers

polymer	$M_W \times 10^3$	M_w/M_n	T_g (°C)
1	35.2	2.9	81
2a	24.3	3.6	114
2b	29.6	3.9	93
2c	11.0	2.4	100
2d	15.5	2.7	61
2e	10.1	2.8	118
2f	10.2	3.0	71
2g	27.3	3.8	105
2h	3.9	1.3	

(KBr, cm^{-1}): 3013, 2959, 2924, 2900, 2835, 1681, 1581, 1504, 1462, 1419, 1331, 1234, 1126, 983, 960, 838, 758, 698, 667. Elemental calcd. for $(C_{34}H_{32}O_6)_n$: C, 76.11; H, 5.97. Found: C, 75.18; H, 5.77.

Copolymer 2g: ^{1}H NMR ($CDCl_3$, δ): 7.6 (s, 1 H), 7.5 (s, 1 H), 7.4 (m, 6 H), 7.04 (d, 4 H), 6.7 (s, 4 H), 5.0 (s, 4 H), 3.9 (s, 12 H). FTIR (KBr, cm^{-1}): 3020, 2960, 2920, 2850, 1584, 1462, 1422, 1328, 1234, 1128, 960. Elemental calcd. for $(C_{34}H_{32}O_6)_n$: C, 76.11; H, 5.97. Found: C, 75.56; H, 5.71.

Copolymer 2h: ^{1}H NMR ($CDCl_3$, δ): 8.4 (m, 4 H), 7.8 (d, 2 H), 7.7 (s, 1 H), 7.5 (m, 4 H), 7.4 (m, 3 H), 6.9 (s, 4 H), 6.8 (d, 2 H), 5.1 (s, 4 H), 3.9 (s, 12 H). FTIR (KBr, cm^{-1}): 3024, 2960, 2922, 2858, 1580, 1506, 1460, 1420, 1330, 1238, 1130, 1082, 962, 750. Elemental calcd. for $(C_{42}H_{36}O_6)_n$: C, 79.24; H, 5.66. Found: C, 78.47; H, 5.45.

Results and Discussion

Synthesis and Characterization. The polymers were synthesized using Wittig polycondensation which requires the use of aromatic dialdehydes with phosphonium salt to form the vinylic bonds in the polymer. The copolymers were isomerized to an all-trans configuration by refluxing the polymer solution in toluene with a catalytic amount of iodine. The structure of the polymers was established by FTIR and ^{1}H NMR. The ^{1}H NMR spectrum confirmed the absence of the cis vinylic around 6.5 ppm. The FTIR spectra showed a band near 965 cm^{-1} due to the C−H stretch of the vinylic units further confirming a trans configuration. The only exception was **2f** with 25% cis configuration.

All the copolymers are readily soluble in chloroform, methylene chloride, tetrahydrofuran, etc. It can be concluded that substitution of the aliphatic spacer by a *m*-xylene unit did not significantly decrease the solubility of the polymers. Gel permeation chromatography (GPC) showed the molecular weight distributions of the polymers (Table 1) are broad, typical of a Wittig type reaction. [2] The low molecular weight of **2h** is due to early precipitation in the polymerization solvents and is accounted for by the steric bulkiness of the 9,10-anthrylene unit.

Thermal Analysis. T_g's of the copolymers were determined by DSC in nitrogen atmosphere at a heating rate of 10 °C/min. Neither a melting point nor any other first-order transition attributed to liquid crystal behavior could be observed in multiple heating and cooling cycles in the range 30−200 °C. As expected, the T_g of **2a** (114 °C) is 30 °C higher than that of **1** because of the introduction of the rigid moiety in the spacer linkage. However, in contrast to earlier results, the structure of the chromophore substituents for the copolymers **2b**−**2e** studied here also affects the measured glass transition temperature, which in previous work[5] had been attributed to the microphase-separated soft block. In the present case, the aromaticity of both chromophore and spacer block reduces the driving force for phase separation. The addition of flexible alkoxy groups substituents on the central phenyl ring of the chromophore decreases T_g; thus, copolymer **2d** has the lowest T_g (61 °C) of the present series because of the plasticization induced by long alkoxy substitution ($-OC_{16}H_{33}$).[12] The introduction of a fluorine atom on the chromophore unit in **2e** increases T_g relative to **2**. Because of the nonlinear structures of **2f** and **2g**, these copolymers have lower T_g's compared to that of **2a**. The lower T_g (71 °C) for **2f** arises because of the significant percentage of cis configuration in this polymer. No T_g was observed in **2h** because of the bulky, rigid 9,10-anthrylene unit at the center of the chromophore. Although **2h** has a relatively low molecular weight (3.9 $\times$ 10^3 g mol^{-1}), the rigidity of the hard segments increased the T_g to above the decomposition temperature of the polymer.

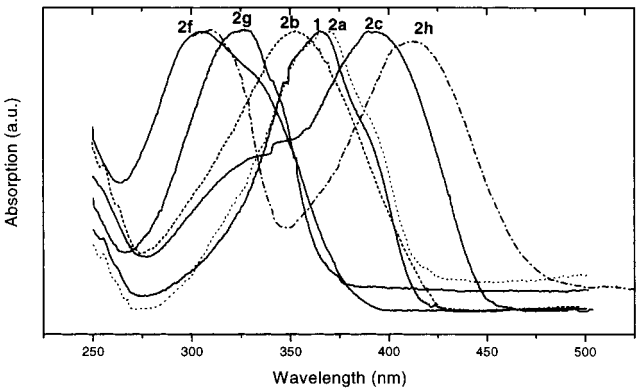

Figure 1. Absorption spectra of **1, 2a, 2b, 2c, 2f, 2g**, and **2h** in chloroform (10^{-5} M) at room temperature.

Table 2. Optical Properties of Copolymers in Chloroform (10^{-5} M)

polymer	λ_{max} (nm) absorption	λ_{max} (nm)[a] emission	φ_f[b]
1	370	439	0.38
2a	370	439	0.42
2b	355	448	0.73
2c	390	450	0.45
2d	395	453	0.48
2e	355	445	0.68
2f	305	435	0.28
2g	325	409	0.12
2h	410	490	0.03

[a] Excited at absorption maximum. [b] 9,10-Diphenylanthracene used as standard.

Solution Optical Properties. The absorption and emission spectra of **2a**−**h** in chloroform (10^{-5}M) were compared to those of the reference copolymer **1** (Figure 1 and Table 2). The absorption and emission maxima and fluorescence quantum yields are listed in Table 2. The absorption spectra are independent of the nature of the spacer unit; both **1** and **2a** show maxima around 370 nm. However, substitutents on the chromophore and the chromophore architecture strongly influence the UV−vis spectra. Compared to **2a**, alkoxy-substituted **2c** and **2d** show large red shifts. The electron-donating methyl substitution in **2b** causes a blue shift. This shift in the UV−vis is due to the twisting of the chromophore induced by the bulky alkyl groups. When electron-donating substitutents are replaced by electron-withdrawing group (**2e**), a blue shift is observed. Copolymer **2h** shows a red shift due to the extended conjugated π-system in the chromophore. Copolymers **2f** and **2g** are blue-shifted compared to **2a**, where π-delocalization is disrupted by ortho and meta linkages. However, **2f** is

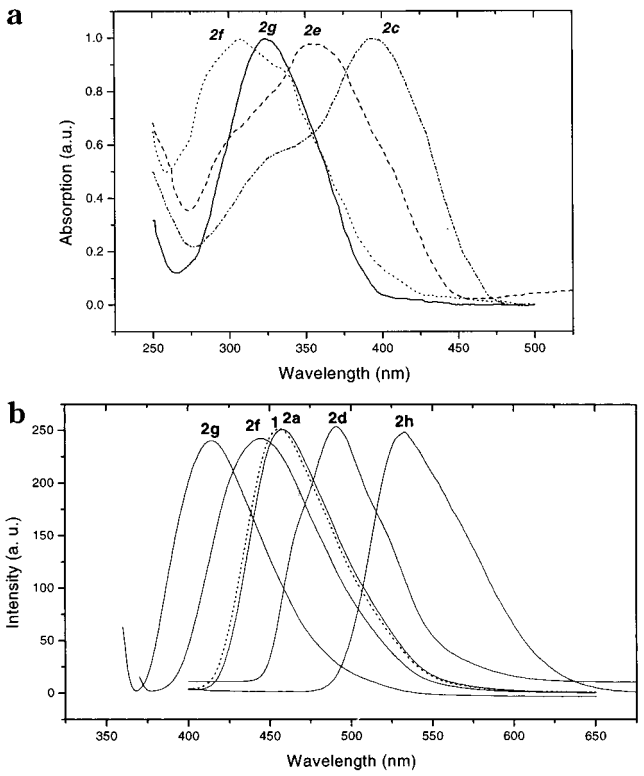

Figure 2. (a) Absorption spectra of **2c, 2e, 2f**, and **2g** thin films at room temperature. (b) Photoluminescence spectra of **1**, **2a, 2d, 2f, 2g**, and **2h** thin films at room temperature.

more blue-shifted than **2g**, despite increased π-delocalization. Similar ortho and meta linkage effects on the UV−vis spectrum have been observed previously.[13]

The emission spectra follow the same trends as the absorption spectra in dilute solution with some variations in **2b, 2e, 2f**, and **2g**. Thus, the emission maximum of **2b** is slightly red-shifted compared to that in **1** or **2a**. This suggests that the excited-state structure for **2b** has a more planar structure than the ground state and this is confirmed by the high quantum yield (ϕ_f = 0.73). The introduction of a fluorine atom **(2e)** also produces a red-shifted emission and a higher quantum yield (Table 2). The probability of nonradiative deactivation of singlet excitons is enhanced by the presence of oxygen atoms in the chromophore.[14] Thus, dialkoxy-substituted PPV has a lower emission quantum yield than that of unsubstituted PPV.[15] However, the introduction of alkoxy groups in **2c** and **2d** did not decrease the quantum yields relative to **2a**. This suggests that the relative position and sequence of oxygen in the extended conjugated chain is a factor in emission quantum yields.[16] Copolymer **2f** has a red-shift emission relative to **2g**. The low quantum yields of in **2f** and **2g** is accounted for by the disruption of conjugation or π-delocalization over the chromophore unit.

Thin Film Optical Properties. The UV−vis spectra of thin films (90 nm) show smaller blue shifts but are characteristically broader compared to those of the solution spectra (Figure 2a and Table 3). This result points to the existence of some solid-state aggregation.[17] The absorption maximum of **2e** is 20 nm blue-shifted relative to that of **2a**. However, its absorption edge (Table 3) is slightly higher than **2a**. The same effect is also observed for **2f** and **2g**. The optical band gaps of the polymers were calculated from the edge location of the respective spectra.

Table 3. Optical Properties of Polymer Films

polymer	λ_{max} (nm) absorption	λ_{max} (nm)[a] emission	absorption edge (nm)	fwhm (nm)
1	368	458	435	62
2a	367	458	435	62
2b	350	455	430	65
2c	390	495	470	62
2d	388	492	470	60
2e	348	463	440	70
2f	307	445	417	77
2g	320	413	397	65
2h	413	533	507	69

[a] Excited at absorption maximum.

Table 4. Electrochemical Properties of Polymer in Solid Films

polymer	E^{red}_{onset} (V)[a]	E^{ox}_{onset} (V)[a]	E^{el}_g (eV)[b]	E^{op}_g (eV)[c]	HOMO (eV)[d]	LUMO (eV)[e]
1	−2.14	0.81	2.95	2.85	−5.61	−2.66
2a	−2.15	0.80	2.95	2.85	−5.60	−2.65
2b	−2.16	0.78	2.94	2.88	−5.58	−2.64
2c	−2.20	0.65	2.85	2.64	−5.45	−2.60
2d	−2.19	0.68	2.87	2.64	−5.48	−2.61
2e	−2.13	0.80	2.93	2.82	−5.60	−2.67
2f	−2.20	0.90	3.10	2.97	−5.70	−2.60
2g	−2.25	1.05	3.30	3.12	−5.85	−2.55
2h	−1.68	0.73	2.41	2.45	−5.53	−3.12

[a] Onset reduction and oxidation potentials vs ferrocene/ferrocenium. [b] Band gaps obtained using: E^{el}_g = LUMO−HOMO. [c] Band gaps calculated from the absorption spectra edges. [d] Determined from the onset oxidation potential (energy level of ferrocene to be −4.8 eV).[25] [e] Determined from the onset oxidation potential (energy level of ferrocene to be −4.8 eV).[26]

The photoluminescence spectra of the films follow similar trends as that of the corresponding solutions. The emissions in the solid state are red-shifted relative to those of the solution state. These shifts are due to intermolecular $\pi-\pi$ interaction of the chromophores.[18] Copolymers **2b**, **2f**, and **2g** show smaller red shifts compared to others, indicating that the planarity of the conjugated moiety controls the $\pi-\pi$ interaction. It should be noted that the emission peaks in films are sharp with the full width at half-maximum (fwhm) less than 70 nm (Table 3). Photoluminescence spectra for polymer **1**, **2a, 2d, 2f, 2g**, and **2h** are shown in Figure 2b.

Electrochemical Properties. Charge injection processes and electronic states of the these copolymers were investigated by cyclic voltammetry.[19,20] From the difference of onset potentials, the band gaps were determined and compared to those obtained from the spectral data[21,22] (Table 4). Examples of typical cyclic voltammograms for **2a, 2c**, and **2g** are given in Figure 3 (scan rate, 50 mA/s). Both the oxidation and reduction processes of these polymers are irreversible. Copolymers **1** and **2a** show the same oxidation and reduction potentials because they contain same chromophore unit. The introduction of a methyl group in **2b** and a fluorine atom in **2e** does not significantly affect redox potentials compared to the case of polymer **2a**. However, the oxidation potentials for alkoxy-substituted **2c** and **2d** are 0.65 and 0.68 V, respectively, lower than that of **2a**. This shows that **2c** and **2d** have a more ready hole injection ability than **2a**, since the oxidation process is correlated with the removal of electrons (or hole injection) from the polymer HOMO levels. Compared to the effect of substituents, main chain variations have more significant effects on the electrochemical properties of these copolymers. Because of the ortho and meta link-

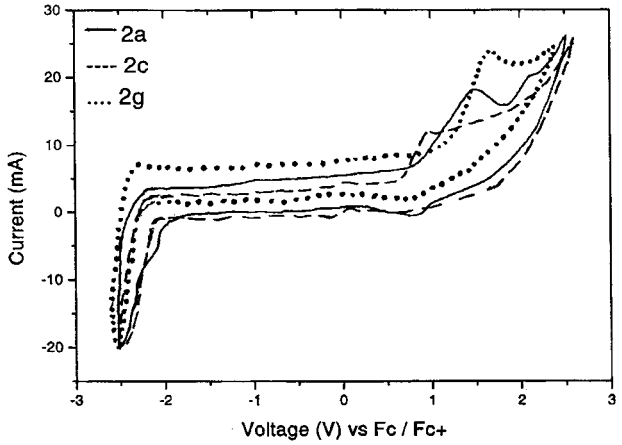

Figure 3. Cyclic voltammograms of polymers **2a**, **2c**, and **2g** at a scan rate of 50 mV/s vs ferrocene/ferrocenium.

ages in the chromophore units, both band gaps and the oxidation potential of **2f** and **2g** are increased in comparison to **2a**. However, replacement of the benzene ring by anthracene in **2h** increases the onset of the reduction potential by 0.47 eV, while the oxidation potential and the band gap decrease. HOMO and LUMO levels were derived from the onset oxidation potentials and reduction potentials, respectively,[23,24] assuming the absolute energy level of ferrocene to be 4.8 eV below the vacuum level.[25,26] The band gaps obtained from the HOMO−LUMO energies (Table 4) are close to those calculated from absorption spectra.

Conclusions

We have reported the synthesis and optical and electrochemical properties of a series of PPV-based alternating copolymers which have relatively high glass transition temperatures. The present results confirm that it is possible to tune the color of emission and to modulate the redox potentials and improve physical properties by changing the substituents and/or backbone structure of the chromophore in an entirely systematic manner.

Acknowledgment. This work was supported by the Air Force Office of Scientific Research (Grant F49620-99-1-002).

References and Notes

(1) Yang, Z.; Sokolik, I.; Karasz, F. E. *Macromolecules* **1993**, *26*, 1188.
(2) Yang, Z.; Hu, B.; Karasz, F. E. *J. Macromol. Sci., Pure Appl. Chem.* **1998**, *A53* (2).
(3) Hu, B.; Karasz, F. E. *Synth. Met.* **1998**, *92*, 157.
(4) Kim, H. K.; Ryu M.-K.; Kim, K.-D.; Lee, S.-M.; Cho, S.-W.; Park, J.-W. *Macromolecules* **1998**, *31*, 1114.
(5) Gürel, E. E.; Pasco, S. T.; Karasz, F. E. *Polymer* **2000**, *41*, 6969.
(6) Sanyo, H.; Hirayama, F. *J. Phys. Chem.* **1983**, *87*, 83.
(7) Campbell, T. W.; McDonald, R. N. *J. Org. Chem.* **1959**, *24*, 1246.
(8) Nakaya, T.; Imoto, M. *Bull. Chem. Soc. Jpn.* **1966**, *39*, 1547.
(9) Kossmehl, G.; Samandari, M. *Makromol. Chem.* **1983**, *184*, 2437.
(10) Nakaya, T.; Tomomoto, T.; Imoto, M. *Bull. Chem. Soc. Jpn.* **1966**, *39*, 1551.
(11) McCoy, R. K.; Karasz, F. E.; Sarker, A.; Lahti, P. M. *Chem. Mater.* **1991**, *3*, 941.
(12) Pasco, S. T.; Lahti, P. M.; Karasz, F. E. *Macromolecules* **1999**, *32*, 6933.
(13) Ahn, T.; Jang, M. S.; Shim, H.-K.; Hwang, D.-H.; Zyung, T. *Macromolecules* **1999**, *32*, 3279.
(14) Attias, A.-J.; Hapiot, P.; Wintgens, V.; Valat, P. *Chem. Mater.* **2000**, *12*, 461.
(15) Woo, H. S.; Graham, S. C.; Halliday, D. A.; Bradley, D. D. C.; Friend, R. H.; Burn, P. L.; Holmes, A. B. *Phys. Rev. B* **1992**, *46* (12), 7379.
(16) Cacialli, F.; Chuah, B. S.; Kim, J. S.; dos Santos, D. A.; Friend, R. H.; Moratti, S. C.; Holmes, A. B.; Brédas, J. L. *Synth. Met.* **1999**, *102*, 924.
(17) Song, X.; Geiger, C.; Leinhos, U.; Perlstein, J.; Whitten, D. G. *J. Am. Chem. Soc.* **1994**, *116*, 10340.
(18) Yamamoto, T.; Sugiyama, K.; Kushida, T.; Inoue, T.; Kanbara, T. *J. Am. Chem. Soc.* **1996**, *118*, 3930.
(19) Osaheni, J. A.; Jenekhe, S. A. *Chem. Mater.* **1995**, *7*, 672.
(20) Peng, Z. H.; Bao, Z. N.; Galvin, M. E. *Chem. Mater.* **1998**, *10*, 2086.
(21) Eckhardt, H.; Shacklette, L. W.; Jen, K. Y.; Elsenbaumer, R. L. *J. Chem. Phys.* **1989**, *91*, 1303.
(22) Wang, L.-H.; Chen, Z.-K.; Kang, E.-T.; Meng, H.; Huang, W. *Synth. Met.* **1999**, *105*, 85.
(23) Peng, Z. H.; Bao, Z. N.; Galvin, M. E. *Chem. Mater.* **1998**, *10*, 2086.
(24) Agrawal, A. K.; Jenekhe, S. A. *Chem. Mater.* **1996**, *8*, 579.
(25) Wu, C.-C.; Sturm, J. C.; Register, R. A.; Tian, J.; Dana, E. P.; Thompson, M. E. *IEEE Trans. Electron Devices* **1997**, *44*, 1269.
(26) Jandke, M.; Strohriegl, P.; Berleb, S.; Werner, E.; Brütting, W. *Macromolecules* **1998**, *31*, 6434.

MA000865X